Petra Seibert, Radek Hofman, Anne Philipp

Possible Consequences of Severe Accidents at the Proposed Nuclear Power Plant Site Lubiatowo near Gdańsk, Poland

Final Report from March 4, 2014

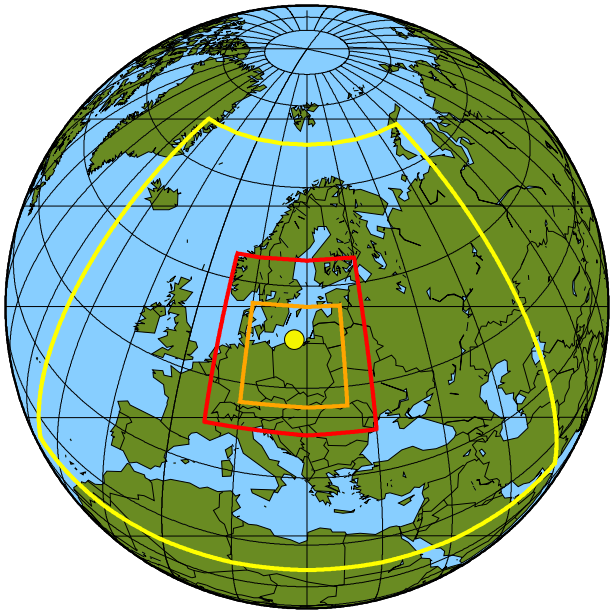

Department of Meteorology and Geophysics
University of Vienna, Austria
March 2014

This publication should be quoted as follows:

Petra Seibert, Radek Hofman, Anne Philipp (2014): Possible Consequences of Severe Accidents at the Proposed Nuclear Power Plant Site Lubiatowo near Gdańsk, Poland. Final Report from March 4, 2014. University of Vienna, Department of Meteorology and Geophysics, Vienna, Austria.

IMPRESSUM

Medieninhaberin und Herausgeberin:

Univ.-Prof. Dr. Petra Seibert
Institut für Meteorologie und Geophysik
Universität Wien
Althanstr. 14
1090 Wien, Austria

URL `http://imgw.univie.ac.at/`

Contents

List of Tables

List of Figures

1 Introduction

Severe accidents in nuclear power plants have a potential to create widespread contamination of the environment. The disasters of Chernobyl in 1986 and Fukushima in 2011 bear evidence of that. Authorities in regions where nuclear power plants are operated need to be prepared for the potential consequences of severe accidents. Public discussion should as well have access to scientifically based information on contamination and possible doses which might be expected in such cases.

Out of these and other considerations, a major project has been carried out in Austria between 2009 and 2012 under the title "flexRISK – Flexible tools for assessment of nuclear risk in Europe" (Seibert et al., 2013; flexRISK team, no date; Arnold et al., 2013; Seibert et al., 2012). In this project, all operating nuclear power plants in Europe and those which were under construction or at least in an advanced planning stage were considered. A severe accident with a large release of radioactivity into the environment was selected among publicly available accident scenarios for each plant. Then, dispersion and dose calculations were performed for a large number (2820) real weather situations. Sample contamination and dose patterns for each reactor unit were published on the web and statistical evaluations were carried out for the major endpoints of the calculations. All this was done on a European scale, as in the case of large accidents, which may release 100% of the noble gases and typical fractions of iodine and caesium exceeding 10% of the respective inventory, relevant contamination is likely to occur at distances of hundreds of kilometres and even beyond.

Poland is one of the European countries which presently do not use nuclear power. However, in recent years, preparations have been advanced towards establishing a nuclear power programme. Possible sites have been selected and a short list of envisaged suppliers of reactors with specific designs is available. In this study, commissioned by Greenpeace Germany, potential consequences of hypothetical accidents at one of the sites proposed, Lubiatowo at the Baltic Sea, have been investigated using the methodology of the flexRISK project. Pertinent technical information about the plant, especially source terms to be investigated, were researched by the Institute of Safety and Risk, University of Natural Resources and Life Sciences in Vienna on behalf of Greenpeace Germany and made available for the present study (Sholly et al., 2014).

The most important differences of the present work compared to the flexRISK project are:

1. For each reactor design, two accidents were considered instead of a single one, one with a very large release and correspondingly low expected frequency, and one with intact containment and thus much smaller release to the environment.

2. Instead of 2820 weather situations, only 86 situations have been simulated. For this reason, statistical evaluations were not carried out.

3. The evaluation domains are smaller but the spatial resolution of the output grid was increased, so that better estimates at distances of ca. 15 to 150 km are obtained.

4. Having learned that the wet deposition algorithm used in the past produced too strong washout, it has been modified to be more realistic.

Figure 1 shows the coarse output domain with the Lubiatowo site.

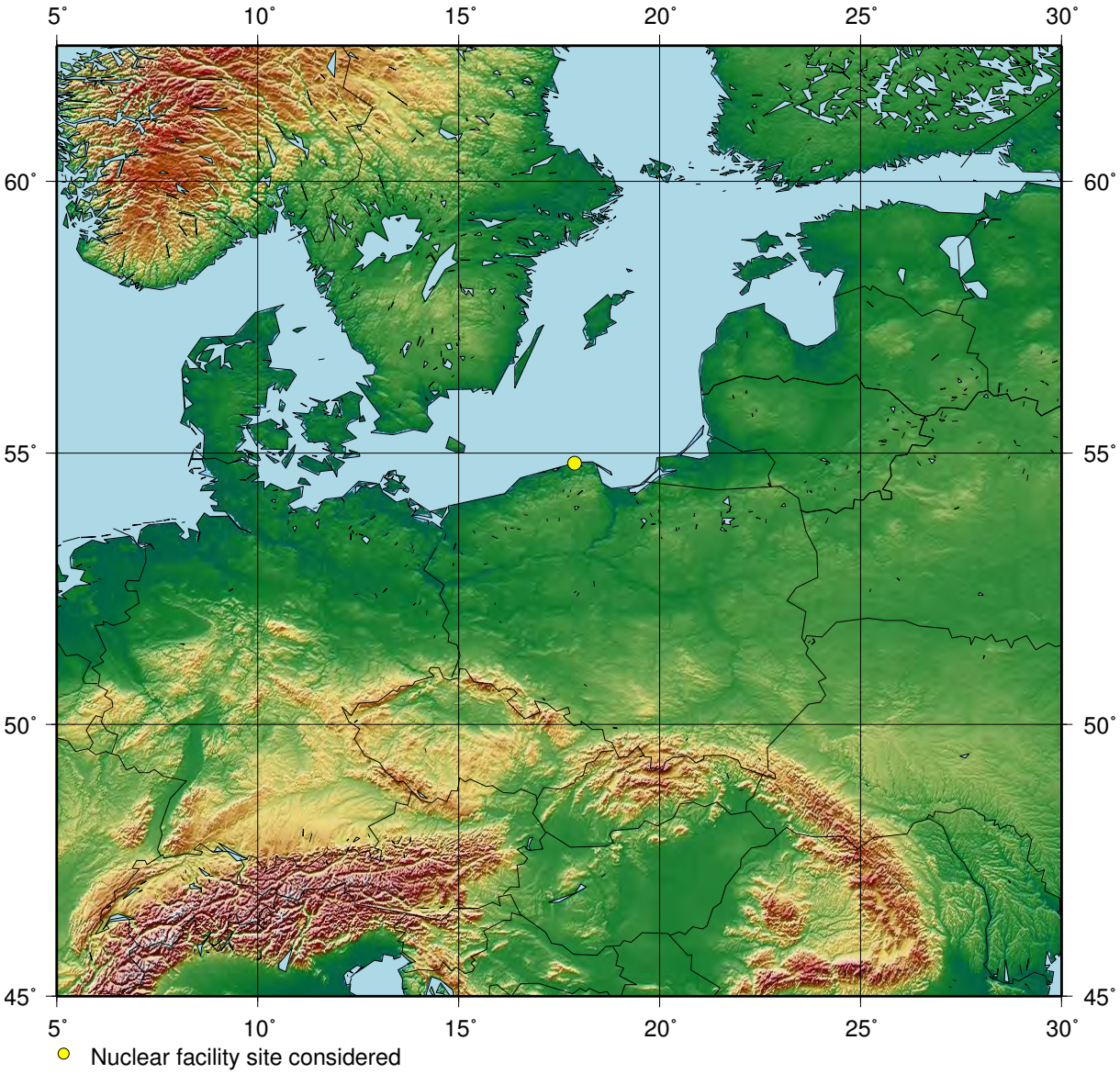

Figure 1: Map of the coarse output domain with the Lubiatowo site marked.

As the methodology is basically the same as in the flexRISK project, it is presented in an abridged fashion in this report. For more details, readers are referred to the flexRISK web site (flexRISK team, no date) and especially the flexRISK Final Report (Seibert et al., 2013).

2 Source term data

The accident sequences and the associated source terms were prepared by Sholly et al. (2014). They selected three possible designs. For practical reasons, each of these designs is treated here as one reactor unit, referred to as Lubiatowo-1 (corresponding to the AP1000), Lubiatowo-2 (EPR), and Lubiatowo-3 (ABWR). Furthermore, for each of the designs, two accident sequences were selected. The first one, here referred to as accident "A", assumes a core-melt accident with the containment remaining intact, leaking at its design rate. The second one, here referred to as accident "B", assumes failure or bypass of the containment and thus very large releases. A brief characterisation of the reactor designs and accidents considered can be found in Table 1.

The source term characteristics are listed in Table 2. The releases of the key nuclide for the thyroid dose, ^{131}I, range between 7 and 91 TBq[1] in the "A" accidents and 0.9 to 1.9 EBq in the "B" cases, thus varying by factor of 100,000. For ^{137}Cs, the key nuclide for effective doses, releases in the "A" cases are in the 1 to 12 TBq range, and in the "B" cases between ca. 100 and 300 PBq, which is a similar variation between the two accident types as in the case of iodine. The release fractions of the "A" accidents of these two key nuclides are on the order of $1 \cdot 10^{-6}$ to $1 \cdot 10^{-5}$, whereas for the "B" accidents they vary between 18 % and 58%. This indicates very clearly the different character of these accidents – only the "B" accidents fall into a class similar to Chernobyl (see, e.g., Davoine and Bocquet (2007)) and Fukushima (see, e.g., Stohl et al. (2012)). Actually, the "B" caesium releases are on the order of one magnitude larger than the current estimates for atmopsheric releases from Fukushima, and the largest ones even exceed the estimate for Chernobyl.

The release shapes are presented in Table 5. All releases are considered to consist of only a single phase (note that phases with releases that are negligible compared to the main phase do not need to be taken into account). A release shape for such a simple release is defined as the time of begin and end of the release and its effective height interval. The duration of the releases is on the order of a few hours. The source term descriptions that were extracted by Sholly et al. (2014) from open sources contain a release height. However, these release heights do not consider building effects or plume rise of hot effluents. As FLEXPART does not model such effects explicitly, it was necessary to replace them by estimated effective release heights. Details are discussed below in Section 3.5.1.

[1] 1 TBq (Terabecquerel) is $1 \cdot 10^{12}$ Bq, 1 PBq (Petabecquerel) is $1 \cdot 10^{15}$ Bq, and 1 EBq (Exabecquerel) is $1 \cdot 10^{18}$ Bq.

Table 1: List of accidents considered with an abridged description and associated estimated frequency of occurrence. The number in the column "Source" refers to the reference number in Sholly et al. (2014). Personal communication from the ISR team, and extracted from Sholly et al. (2014).

Release type	Reactor type	Accident	Frequency (a^{-1})	Source
1A	Westinghouse AP1000	Severe accident with an intact containment (IC) and release at design containment leakage rate.	2.21E-07	[25]
1B	Westinghouse AP1000	Severe accident with a containment bypass scenario (BP) resulting from steam generator tube failure (either as the initiating event, or resulting from failure of one or more tubes due to high temperature during accident progression).	1.05E-08	[25]
2A	Areva European Pressurized Reactor	Severe accident with an intact containment, and release at design containment leakage rate. It considers deposition in the annulus and fuel/safeguards buildings without building ventilation.	1.44E-07	[30]
2B	Areva European Pressurized Reactor	Severe accident with small interfacing system LOCA, without fission product scrubbing and fission product deposition in fuel/safeguards building.	3.70E-09	[30]
3A	Hitachi-GE Advanced Boiling Water Reactor	Severe accident, with the containment staying intact. The release to the environment happens at design containment leakage rate.	2.10E-07	[34]
3B	Hitachi-GE Advanced Boiling Water Reactor	"Case 13": The accident is assumed to occur during shutdown, with an open RPV, when cooling of the core is lost. In this scenario fission products have a direct path to the environment via the open RPV and containment.	1.20E-09	[34]

Table 2: Releases of key radionuclides for the assumed accident sequences (absolute and release fractions). The colum "U-A" refers to the pseudo-unit and the accident. More information on the accident types is found in Table 1. Source: Sholly et al. (2014).

U-A	Xe-133		I-131		Cs-137		Te-132		Sr-90		Ru-106	
	PBq	fraction	PBq	fraction	PBq	fraction	PBq	fraction	PBq	fraction	PBq	fraction
1A	19	2.6e-3	4.3e-2	1.2e-5	4.8e-3	1.2e-5	4.1e-3	8.1e-7	3.3e-3	1.1e-5	2.3e-2	1.3e-5
1B	7030	1.000	1593	0.447	114	0.272	83	0.016	1.1e+0	3.6e-3	79	0.045
2A	30	2.8e-3	6.9e-3	1.3e-6	1.0e-3	1.1e-6	1.2e-2	1.6e-6	2.1e-4	3.4e-7	1.1e-2	2.1e-6
2B	8747	0.818	915	0.178	163	0.178	989	0.135	15	0.024	401	0.076
3A	357	0.044	9.1e-2	2.3e-5	1.2e-2	2.3e-5	3.0e-2	5.3e-6	0	0	0	0
3B	8114	1.000	1945	0.490	298	0.580	170	0.030	2.9e-1	7.5e-4	4.0e-3	1.9e-6

3 Dispersion calculations

3.1 Dispersion model

The dispersion calculations were carried out with the Lagrangian particle model FLEXPART (Stohl et al., 1998, 2005; Forster et al., 2007; Stohl et al., 2010) which is used worldwide and freely available (FLEXPART Developer Team, no date). This model was used in the RISKMAP project (Andreev et al., 1998, 1999; Hofer et al., 2000), in flexRISK (Seibert et al., 2013), (Wenzel et al., 2012), but also, for example, for an assessment of the Fukushima sourceterm (Stohl et al., 2012). The model is designed for mesoscale and long-range dispersion. Therefore, results on the local scale (closer than about 15 km from the source) should not be considered.

The model version used is a slightly improved form of the version used for flexRISK and thus based on an unofficial version of FLEXPART 8.1 which is close to FLEXPART 8.2 for which documentation is available (Stohl et al., 2010). The modifications made for flexRISK are

- termination of a run if the total airborne mass of all species falls below 0.5% of their initial values;
- writing out only the sum of dry and wet deposition, not both components separately;
- writing out incremental deposition instead of accumulated deposition.

Already in flexRISK, attention was given to the wet deposition scheme. This was switched with FLEXPART 8 from a simple scheme which scavenged the whole atmospheric column with a fraction depending on the precipitation rate to a scheme with separate consideration of in-cloud and below-cloud scavenging. While initial problems with this more sophisticated scheme could not be solved in flexRISK, more insight was gained recently (Seibert and Philipp, 2013) and we thus could implement a modified version of this scheme. The same modification has become operational in the FLEXPART-WRF version 3.1 (Brioude et al., 2013) and shall become operational in the upcoming official version FLEXPART 9.2. It was also used and described in detail in a recent analysis of Fukushima consequences (Arnold et al., 2014).

3.2 Model setup

FLEXPART can produce output on a nested domain structure. Like in flexRISK, this feature was used. However, both domains were reduced in size while the grid cell size was reduced. For the coarse domain, an output grid resolution of approx. 12 km was used instead of 1° (ca. 100 km) in flexRISK. The fine domain has a grid resolution of ca. 3 km instead of ca. 10 km. This allows for a much better resolution of sharp gradients and narrow plumes and considerably improves the usability of the output in the near range, shifting the limit where the fine-grid output resolution is adequate from originally 50 to 100 km to about 15 km. Table 3 and Figure 2 give an overview of the input and output domains.

Table 3: Specification of FLEXPART domains (domain borders, grid cell sizes, grid cell numbers). "outgrid" stands for output grid, x values refer to geographical longitude, y values to latitude. The border coordinates refer to the outermost grid points in the case of the meteorological fields, whereas for the output domains, they indicate the edges of the outermost grid cell.

Domain	x_{min}	x_{max}	y_{min}	y_{max}	Δx	Δy	n_x	n_y	$n_x n_y$
meteo fields	−25.50	60.00	24.75	75.00	0.75	0.75	114	67	7,638
coarse outgrid	5.00	30.00	45.00	62.50	0.20	0.10	125	175	21,875
fine outgrid	10.00	26.00	48.00	58.00	0.040	0.025	400	400	160,000

3.3 Meteorological input

Meteorological input data used are ERA-Interim, the re-analysis from ECMWF (Dee et al., 2011) which was extracted on a geographical grid with 0.75° horizontal resolution (at 50°N, this corresponds to 83 km × 54 km), and at 3 h temporal resolution (4DVAR analyses and 3-h forecasts) at all model levels. These are the same data as used in flexRISK. The domain is shown in Figure 2 and numerically defined in Table 3. There are two reasons why the meteorological input data being used cover a much larger domain than the output. Firstly, the data were already available in this form from flexRISK, but more importantly, radioactivity is not lost

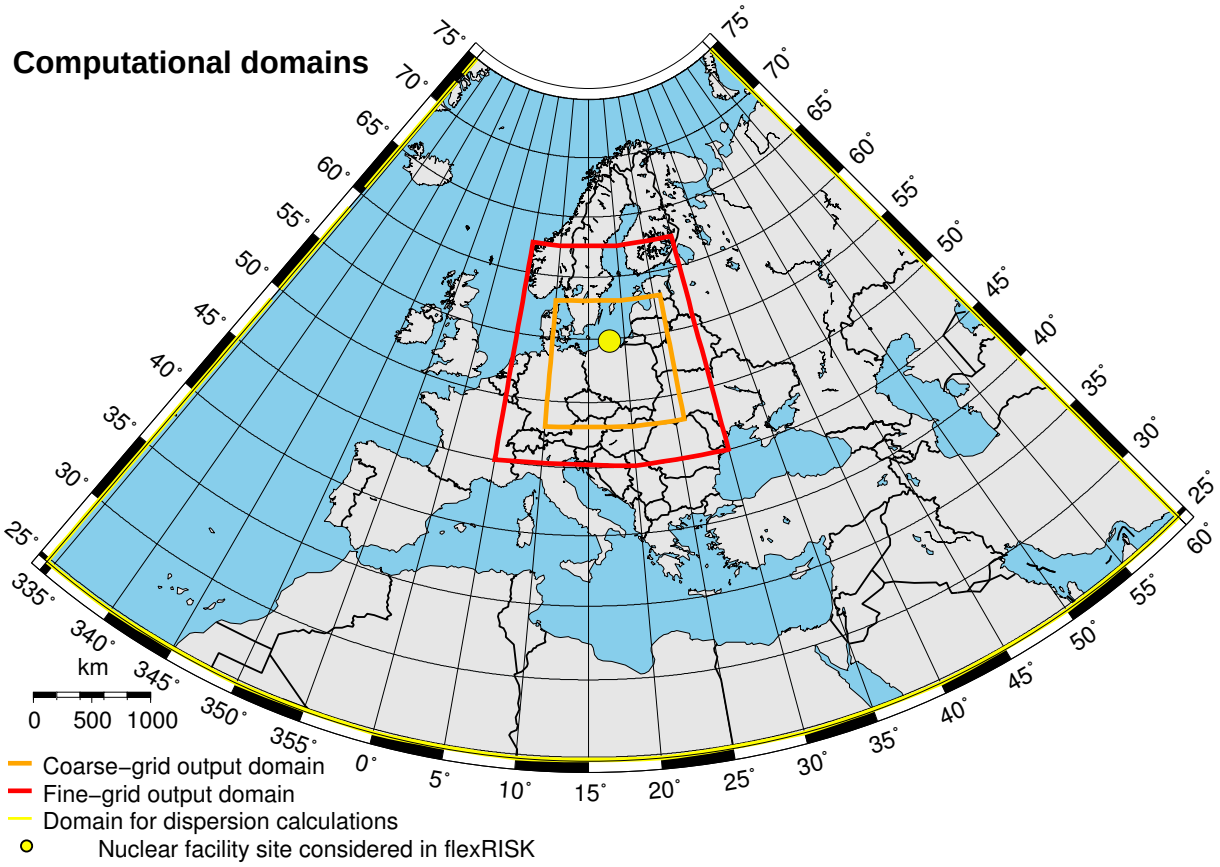

Figure 2: Domains used in the FLEXPART calculations.

Table 4: Values of key internal FLEXPART parameters.

Parameter	Value
Output frequency	3,600 s (1 h)
Output integration time	3,600 s (1 h)
Output sampling interval	300 s (5 min)
Particle splitting	no
Synchronisation time step	300 s (5 min)
Time step	Lagrangian time scale / 3.0
Vertical time step	time step / 4
Subgrid terrain effect parameterisation	on
Convection	on
Units	mass units for source and receptor
Number of output layers	1
Output layer height	150 m
Minimum mixing height	100 m
Number of particles per run	1,500,000

easily from the model, for example when it is transported along curved trajectories which first leave and then re-enter the output domain.

The resolution of the meteorological data is much coarser than that of the output grid. For a Lagrangian model, this is not a problem in principle. Bilinear interpolation from grid nodes to particle positions is applied. The high output resolution allows to reproduce sharp gradients at the plume borders and reduces artificial spreading and dilution. However, one has to be aware that meteorological phenomena at scales on the order of 150 km and finer won't be resolved. For the coastal Lubiatowo site, this means specifically that land-see breeze circulations are not contained in the model, and also influences of the sea/land contrast on turbulence are only roughly represented. Therefore, the present simulations cannot replace a meso-gamma-scale dispersion calculation which would be desired especially for the regions within ca. 15 to 50 km from the site. This holds even more for the local scale (<15 km).

3.4 Internal parameters of FLEXPART

The setting of the internal parameters of FLEXPART is listed in Table 4. Note that output is now produced with 1-hourly resolution (as compared to 3 h in flexRISK) to give more exact dose values at shorter distances. In response to the fine resolution of the output, both spatially and temporally, the number of computational particles per run has been set to 1.5 mio (compared to 250,000 in flexRISK). Convection has been enabled. The other settings are as in flexRISK.

3.5 Releases

In our approach, the dispersion model does not directly calculate all relevant radionuclides. Instead, it calculates the dispersion and deposition of two tracer species, one for noble gases which undergoes neither dry nor wet deposition or other changes, and an aerosol species which is deposited to the ground by dry deposition and through wet scavenging (washout by rain and snowfall). The source strength is set to unity for both species and results are scaled according to

nuclide-specific source terms in the postprocessing (see Section 4). What needs to be known for the dispersion calculation is the duration and effective height of the release. Both are listed in Table 5. Note that the simulation starts with the beginning of the release – the time between stop of chain reaction and beginning of the release is only used for decay correction in postprocessing. All releases considered contain only a single (major) release phase.

3.5.1 Effective release heights

Sholly et al. (2014) include release heights in their accident descriptions which come from the original sources. These are to be considered heights above ground of physical release locations in the reactor building.

In standard accident consequence codes aimed at the near range, plume rise due to the heat content of releases and initial plume widening through building-induced turbulence is usually considered. However, FLEXPART does not have corresponding modules and thus *effective release heights* need to be specified in the input. We did this in discussion with one of the authors of Sholly et al. (2014), in the form of an educated guess. FLEXPART allows to specify vertical ranges for the release. For most accident sequences, we have just widened the given release height moderately. Table 5 includes the original release heights and the effective release heights used as input to FLEXPART. For the 1B and 3B sequences the effluents will be hot and thus the effective release height was set to the interval from the physical release height up to 100 m. It should be noted that the release height is important mainly for the near range – after some time of dispersion, the activity will be well mixed over the whole atmospheric boundary layer.

Table 5: Release shapes for the different types of accidents. For the accident type, refer to Table 1. The release shape is defined by the time of the release, from t_1 to t_2, measured from the stop of the chain reaction, and the effective release height interval from h_1 to h_2. The release height given in the accident analyses is provided as column "h". Source: Sholly et al. (2014)

Accident type		t_1 (s)	t_2 (s)	h_1 (m)	h_2 (m)	h (m)
1A	AP1000 SA, normal containment leakage rate	900	8100	30	40	35
1B	AP1000, steam-generator tube failure	12600	24600	15	100	15
2A	EPR SA, normal containment leakage rate	16200	68400	30	40	34.75
2B	EPR, small interfacing system LOCA	28080	39240	10	100	10
3A	ABWR SA, normal containment leakage rate	900	8100	35	45	37.7
3B	ABWR, Case 13	12600	24600	0	40	5

3.6 Deposition

Table 6 lists the parameters related to the deposition, both wet and dry.

As already mentioned in Section 3.1, the wet deposition scheme in FLEXPART underwent some changes in the past years. The present calculations use the new scheme which discerns between in-cloud and below-cloud scavenging, with several fixes. Compared to the simple scheme used

Table 6: Parameters governing the deposition of the aerosol species.

Parameter	Value
Half-life	infinite (no on-line decay)
Wet deposition parameter A (below cloud)	$2.0 \cdot 10^{-6}$
Wet deposition parameter B (below cloud)	0.62
Wet deposition parameter A (no cloud diagnosed)	$2.0 \cdot 10^{-5}$
Wet deposition parameter B (no cloud diagnosed)	0.8
Wet deposition parameter C (in cloud)	0.125
Wet deposition parameter D (in cloud)	0.64
Density	$2.0 \cdot 10^{-3}$ kg m^{-3}
Mean diameter	$4.0 \cdot 10^{-7}$ µm
Log variation of diametre	0.3

in older FLEXPART versions and in flexRISK, we have more wet deposition parameters. The "below-cloud" and the "no cloud diagnosed" schemes calculate the washout rate as

$$W = A\, I^B \tag{3.1}$$

where A is the washout rate in s^{-1} and I is the precipitation rate in mm h^{-1}.

The "in-cloud" scheme calculates in principle

$$W = C\, I^D\, H^{-1} \tag{3.2}$$

where H is the cloud thickness in m. The parameters A, B, C, D are given in Table 6. Furthermore, the in-cloud washout rate is limited to the value resulting from Eq. 3.1 – if a very shallow cloud is diagnosed, the value from Eq. 3.2 might become too high. The details of the new scheme (without the fixes!) are explained introduced in Stohl et al. (2010) and more details on the fix are found in Arnold et al. (2014).

3.7 Dates

The period covered is the whole year of 1995. In RISKMAP (Andreev et al., 1998, 1999; Hofer et al., 2000), it was shown that in this year flow directions around the Alps are close to their climatological frequencies, so this year can be considered as an approximation to the climatology for Central Europe.

There are 86 dates in the year 1995 for which runs were performed, distributed evenly over the seasons and the time of the day. The duration of each run is 14 days. A new run is started every 4 d 1 h 32 min. (The last two of the 88 starting dates of the previous RISKMAP data set don't finish within the year 1995 and the 15 d run length, so they are skipped).

With the three reactor designs and two accident scenarios per design, a total of 516 runs resulted. They take about 2 h of CPU time each (without convection, the run time would be around 1 h). The model output (compressed) occupies about 50 GB, and postprocessed data (contamination, doses, graphics files) occupy another 50 GB.

4 Postprocessing

4.1 Endpoints

In a postprocessing step, the raw FLEXPART output is transformed into the products for the endpoints of the calculation. These are:

1. Ground contamination with ^{137}Cs at the end of the simulation ($\mathrm{Bq\,m^{-2}}$), as data file and as image
2. Air contamination with ^{131}I, integrated over the duration of the simulation ($\mathrm{Bq\,s\,m^{-3}}$), as data file and as image
3. Sequences of 1-h mean concentrations of ^{131}I, as movie
4. Thyroid dose from inhalation of iodine and tellurium isotopes during 7 d of exposure (mSv) – relevant for administration of stable iodine, as data file and as image
5. Effective dose for 7 d of exposure, all nuclides, inhalation, groundshine and cloudshine pathways (mSv) – relevant for sheltering, as data file and as image
6. Effective dose for 30 d of exposure, all nuclides, only from groundshine (mSv) – relevant for temporary relocation of population, as data file and as image
7. Effective dose for 1 a of exposure and lifetime (i.e., 50 a), inhalation, groundshine, and cloudshine pathways (mSv) – relevant for comparison with general radiation protection guidelines, as data file and as image.

The doses were calculated for children (below one year of age; lifetime dose not calculated) and adults. Note that the ingestion pathway is not considered even though it can be an important contribution. The reason is that a realistic calculation is not possible with the diverse origins of foodstuffs that are consumed nowadays, and the complicated time dependence (interaction with the vegetation cycle, contamination in agricultural products changing with time, etc.).

All images are made available to the commissioning entity through the project web site, both in screen-quality (gif format) for online viewing, and as high-quality PDFs. Movies of the 1-hourly concentration clouds are in mp4 format.

4.2 From tracer to activity

Activities are obtained by multiplying the tracer concentrations with the inventory of the respective nuclides and then decay-corrected. The inventories are listed in Sholly et al. (2014) and were transmitted, together with all other relevant input data, as a set of spreadsheets.

The iodine data and images are decay-corrected under the assumption that the tracer concentration (which is unaffected by decay) remains constant throughout the 1-h averaging interval for the output. This is the reason why the 1-h interval gives better accuracy than a 3-h interval. For details of the calculation, see Seibert et al. (2013).

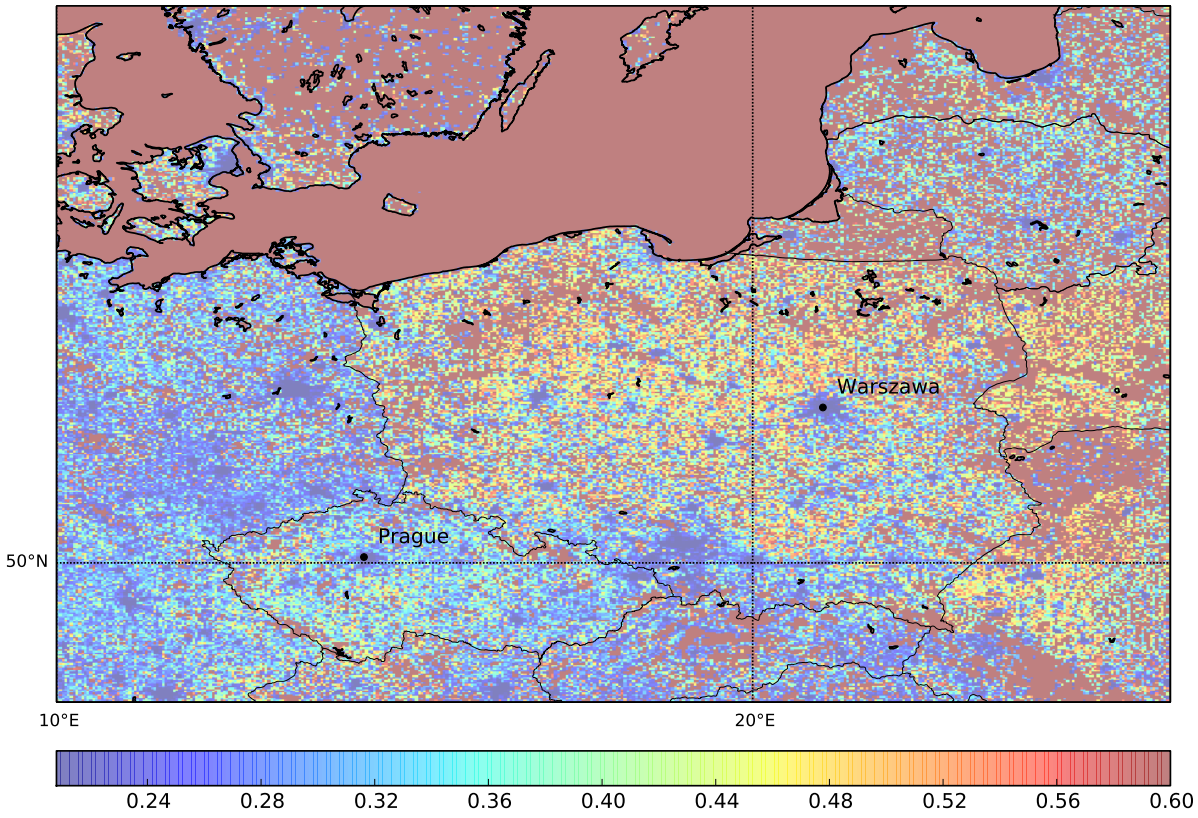

Figure 3: Shielding factors for groundshine (fine domain). Raw doses are multiplied with this factor to obtain the dose for the time spent indoors.

4.3 Dose calculation

The dose calcuation exactly follows the procedures laid out in Seibert et al. (2013, Section 4.3) and are only summarised here. Contributions from 15 nuclides are considered (caesium [134,136,137], iodine [131,132,133,135], rubidium-88, ruthenium [103,106], strontium [88,89] and tellurium-132 as well as the two noble gas nuclides krypton-88 and xenon-135). Decay chains originating from ^{131m}Te and ^{133}I are considered.

The inhalation and cloud-shine dose factors are multiplied with time-integrated concentrations of the respective nuclides in air, the groundshine dose factors are multiplied with time-integrated surface contamination values. A dose reduction factor representing shielding through surface roughness and migration into the ground is considered for the groundshine dose integrated over 1 year (factor of 0.8) and lifetime doses (factor of 0.5). Note that lifetime doses are integrated over 50 years for adults. A shielding factor is used for long-term doses (1 a and lifetime) which considers the protection through buildings while staying indoor. The protection quality of buildings is modelled as a function of population density (better shielding in urban buildings), as can be seen in Figure 3 which shows the groundshine shielding factor. As a consequence, maps of these long-term doses exhibit some spatial scatter over land, corresponding to the population density.

Two types of doses are calculated, the thyroid organ dose and effective dose. The thyroid dose is needed to assess the applicability of the countermeasure of taking stable iodine tablets which, if

taken in time, block the accumulation of radioactive iodine in the thyroid. In Austria, a thyroid dose obtained from 7 d of exposure to contaminated air is considered. Other countries may apply different times, such as 2 d or 5 d. However, as a consequence from the complex and long-lasting Fukushima accident, too short times are considered problematic. Effective doses are calculated according to ICRP 60 (ICRP, 1991).

The dose calculation takes about 5 to 10 min of CPU time per case. In addition, with the large number of output grid cells (ca. 180,000), more than 25 GB of memory (RAM) is needed for each calcuation thread.

5 Results

5.1 Interpretation of logarithmic scales

Contamination and dose values vary by orders of magnitude between locations close to the source and far away. Therefore, logarithmic dose and contamination scales are used in images. Only every 5th interval is annotated on the colour bars in the figure legends, for lack of space. Table 7 shows the values for intermediate intervals which are not annoted in the legends.

Table 7: Numerical values which correspond to intermediate intervals in logarithmic scales. Lines corresponding to four intermediate values used in the colour scales in bold. From Seibert et al. (2013).

Interval	Sample values			
0	**1.00**	**10.0**	**100.**	(annotated)
1	1.26	12.6	126.	
2	**1.58**	**15.8**	**158.**	
3	2.00	20.0	200.	
4	**2.51**	**25.1**	**251.**	
5	3.16	31.6	316.	
6	**3.98**	**39.8**	**398.**	
7	5.01	50.1	501.	
8	**6.31**	**63.1**	**631.**	
9	7.94	79.4	794.	
10	**10.00**	**100.0**	**1000.**	(annotated)

5.2 Contamination and dose values for comparison

In order to make the absolute values of contamination and doses better understandable, some reference values are useful.

For the ^{137}Cs deposition, values used after the Chernobyl disaster by the Soviet authorities can be useful (Table 8). Furthermore, the present level of fallout from the atmospheric nuclear bomb tests, in Austria (and similar elsewhere in Central Europe), was on the order of 2 kBq Cs-137 m^{-2} in the mid-1990ies (Bossew et al., 1996). In Austria, the mean contamination from Chernobyl was about 20 kBq Cs-137 m^{-2} with maxima exceeding 100 kBq Cs-137 m^{-2}. These values led to extensive agricultural countermeasures (Bundeskanzleramt, Sektion VII, 1988).

The maximum concentration of ^{131}I (aerosol-bound only, not including gaseous I_2) in Vienna at the time of the Chernobyl accident was 1.5 nCi m^{-3}, corresponding to about 60 Bq m^{-3} (Bundeskanzleramt, Sektion VII, 1988). This source does not provide the time integral, however, from a figure it can be estimated roughly to be on the order of $2 \cdot 10^6$ Bq s m^{-3}.

As a yardstick for doses, intervention levels for countermeasures are important. Table 9 lists some pertinent levels. Additionally, annual doses may be compared on one hand with the general dose limit for members of the public of 1 mSv per year (from artificial radioactive sources, not related specifically to accidents) according to Council Directive 96/29/Euratom, or

with Austrian intervention levels before 2007, which applied thresholds for the first-year dose (including ingestion, which is not considered here) of 2.5, 25 and 250 mSv.

Table 8: Deposition levels in areas contaminated by the Chernobyl accident (Shevchik and Gurachevsky, 2006). From Seibert et al. (2013).

Zone	Effective dose (mSv/a)	Cs-137 ($kBqm^{-2}$)	Sr-90 ($kBqm^{-2}$)	Pu-238, Pu-239, Pu-240 ($kBqm^{-2}$)
Zone of regular radiation control	<1	37-185	5.55-18.5	0.37-0.74
Zone with the right to resettlement	1-5	185-555	18.5-74	0.74-1.85
Zone of subsequent resettlement	>5	555-1,480	74-111	1.85-3.7
Zone of primary resettlement	>5	>1,480	>111	>3.7
Zone of evacuation (exclusion zone)	Territory around Chernobyl NPP, from which population was evacuated in 1986			

Table 9: Intervention levels for selected intervention measures, different sources. Austria – Lebensministerium (2007), Germany – SSK (2008), IAEA – IAEA (2011). Levels for sheltering refer to effective dose in 7 d, for temporary relocation to effective dose in 30 d, and for iodine prophylaxis to thyroid dose in 7 d (all with specific pathway assumptions). Adapted from Seibert et al. (2013).

Measure	Age group	Austria	Germany	IAEA
Sheltering	Children, pregnant women	1 mSv	10 mSv	100 mSv^{+}
	Adults	10 mSv	10 mSv	100 mSv
Temporary relocation	Children	30 mSv		
	Adults	30 mSv		
Iodine prophylaxis	Children	10 mSv	50 mSv	50 mSv
	Adults up to 40 years	100 mSv	250 mSv	50 mSv*
	Adults over 40 years	500 mSv	**	

$^{+}$ Fetuses

* Before: 100 mSv avertable dose

** Adults over 45 years should not take the iodine tablets at all

5.3 Accidents with intact containment

The accident sequences with intact containment and no bypass ("A" accidents) produce typical maximum ground contamination values[1] on the order of 1 kBq Cs-137 $m^{-2}$and maximum time-integrated ^{131}I concentrations on the order of $1 \cdot 10^6$ kBq Cs-137 m^{-2}. This is comparable with Austria after Chernobyl in areas without precipitation during the passage of the radioactive cloud. Correspondingly, doses remain below the intervention levels, for example the 7-d thyroid doses for children rarely exceed 1 mSv and stay clearly below the 10 mSv limit. Note that this does not mean that countermeasures would not be needed close to the reactor within the emergency planning zone. 1-year effective doses would remain below 1 mSv – however, including the ingestion path which is not considered in our calcuations and in the absence of countermeasures, the 1 mSv general public dose limit can probably be exceeded for people who consume locally produced foods. This situation would thus not constitute a severe nuclear emergency outside

[1]Maximum values discussed always refer to the region covered by our methodology, thus excluding the typical emergency planning zone (EPZ) of ca. 10-20 km radius.

the EPZ, although it can be assumed that intensified sampling of environmental media, fodder and foodstuffs would be considered appropriate in a larger environment. Especially if the accident progression is unclear, precautionary countermeasures might also be considered, such as activation of emergency management bodies and procedures, or measures for the agricultural sector (e.g., sending animals into stables).

5.4 Accidents with very large releases

5.4.1 Overview of possible contamination patterns

Figure 4 gives an overview over all meteorological situations studied. The more severe release from the pseudo-unit 1 is used, but this serves just as an example. The purpose of this overview is to illustrate the wide range of possible contamination patterns. There are cases where the plume remains rather narrow and goes rather straight into one direction. Then there are many cases where after some time the weather pattern changes and large parts or even the whole domain receives contamination at low levels, such as in blue (corresponding to less than than the present nuclear bomb fallout) or sometimes light green (corresponding to Chernobyl fallout in many parts of Central Europe). The plume itself is usually in the orange, red or pink colours (above 100 kBq Cs-137 m^{-2}). The red colours show areas with severe consequences, where resettlement would be considered or – towards the pink colours – required. Due to the occurrence of precipitation, deposition maxima can occur in isolated patches, and it is clearly seen that red colours can be reached practically everywhere on this domain.

Graphical overview of all 86 cases

Below, the ^{137}Cs deposition for all 86 cases is shown for the "1B" release on the coarse domain. The colour bar is included only once at the beginning to save space.

Figure 4: ^{137}Cs deposition for all cases, "1B" release, coarse domain.

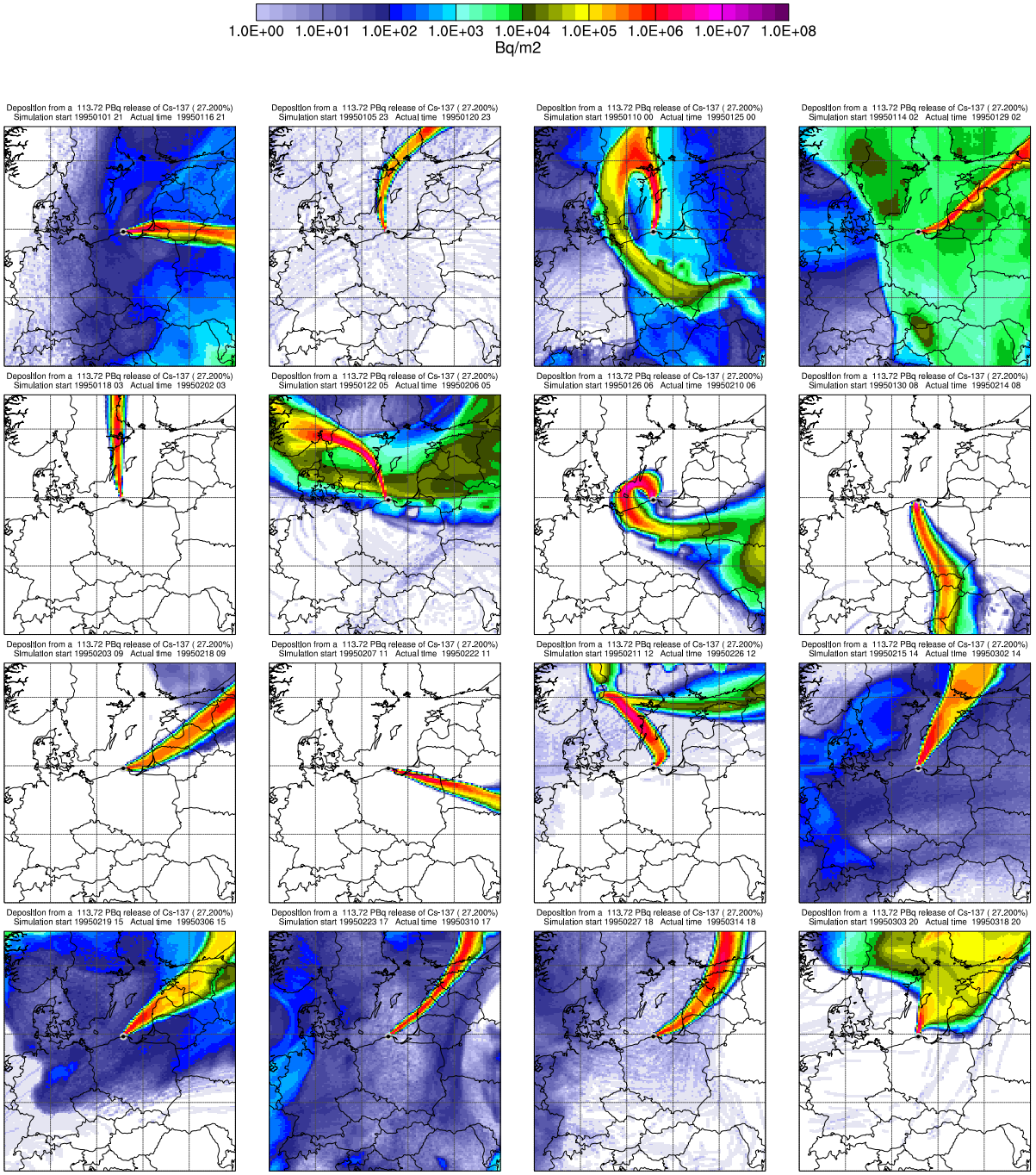

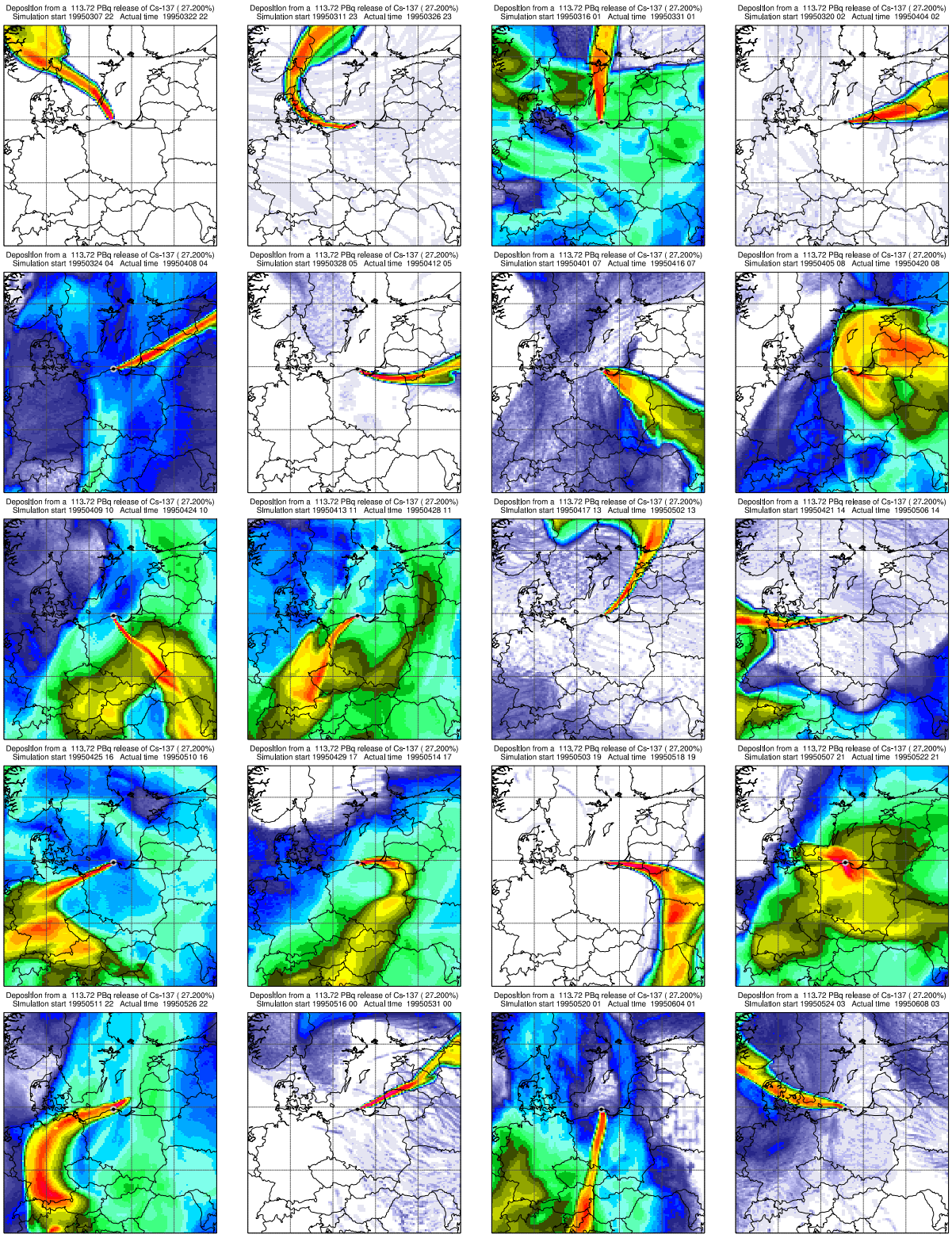
Deposition from a 113.72 PBq release of Cs-137 (27.200%)
Simulation start 19950307 22 Actual time 19950322 22
Deposition from a 113.72 PBq release of Cs-137 (27.200%)
Simulation start 19950311 23 Actual time 19950326 23
Deposition from a 113.72 PBq release of Cs-137 (27.200%)
Simulation start 19950316 01 Actual time 19950331 01
Deposition from a 113.72 PBq release of Cs-137 (27.200%)
Simulation start 19950320 02 Actual time 19950404 02
Deposition from a 113.72 PBq release of Cs-137 (27.200%)
Simulation start 19950324 04 Actual time 19950408 04
Deposition from a 113.72 PBq release of Cs-137 (27.200%)
Simulation start 19950328 05 Actual time 19950412 05
Deposition from a 113.72 PBq release of Cs-137 (27.200%)
Simulation start 19950401 07 Actual time 19950416 07
Deposition from a 113.72 PBq release of Cs-137 (27.200%)
Simulation start 19950405 08 Actual time 19950420 08
Deposition from a 113.72 PBq release of Cs-137 (27.200%)
Simulation start 19950409 10 Actual time 19950424 10
Deposition from a 113.72 PBq release of Cs-137 (27.200%)
Simulation start 19950413 11 Actual time 19950428 11
Deposition from a 113.72 PBq release of Cs-137 (27.200%)
Simulation start 19950417 13 Actual time 19950502 13
Deposition from a 113.72 PBq release of Cs-137 (27.200%)
Simulation start 19950421 14 Actual time 19950506 14
Deposition from a 113.72 PBq release of Cs-137 (27.200%)
Simulation start 19950425 16 Actual time 19950510 16
Deposition from a 113.72 PBq release of Cs-137 (27.200%)
Simulation start 19950429 17 Actual time 19950514 17
Deposition from a 113.72 PBq release of Cs-137 (27.200%)
Simulation start 19950503 19 Actual time 19950518 19
Deposition from a 113.72 PBq release of Cs-137 (27.200%)
Simulation start 19950507 21 Actual time 19950522 21
Deposition from a 113.72 PBq release of Cs-137 (27.200%)
Simulation start 19950511 22 Actual time 19950526 22
Deposition from a 113.72 PBq release of Cs-137 (27.200%)
Simulation start 19950516 00 Actual time 19950531 00
Deposition from a 113.72 PBq release of Cs-137 (27.200%)
Simulation start 19950520 01 Actual time 19950604 01
Deposition from a 113.72 PBq release of Cs-137 (27.200%)
Simulation start 19950524 03 Actual time 19950608 03

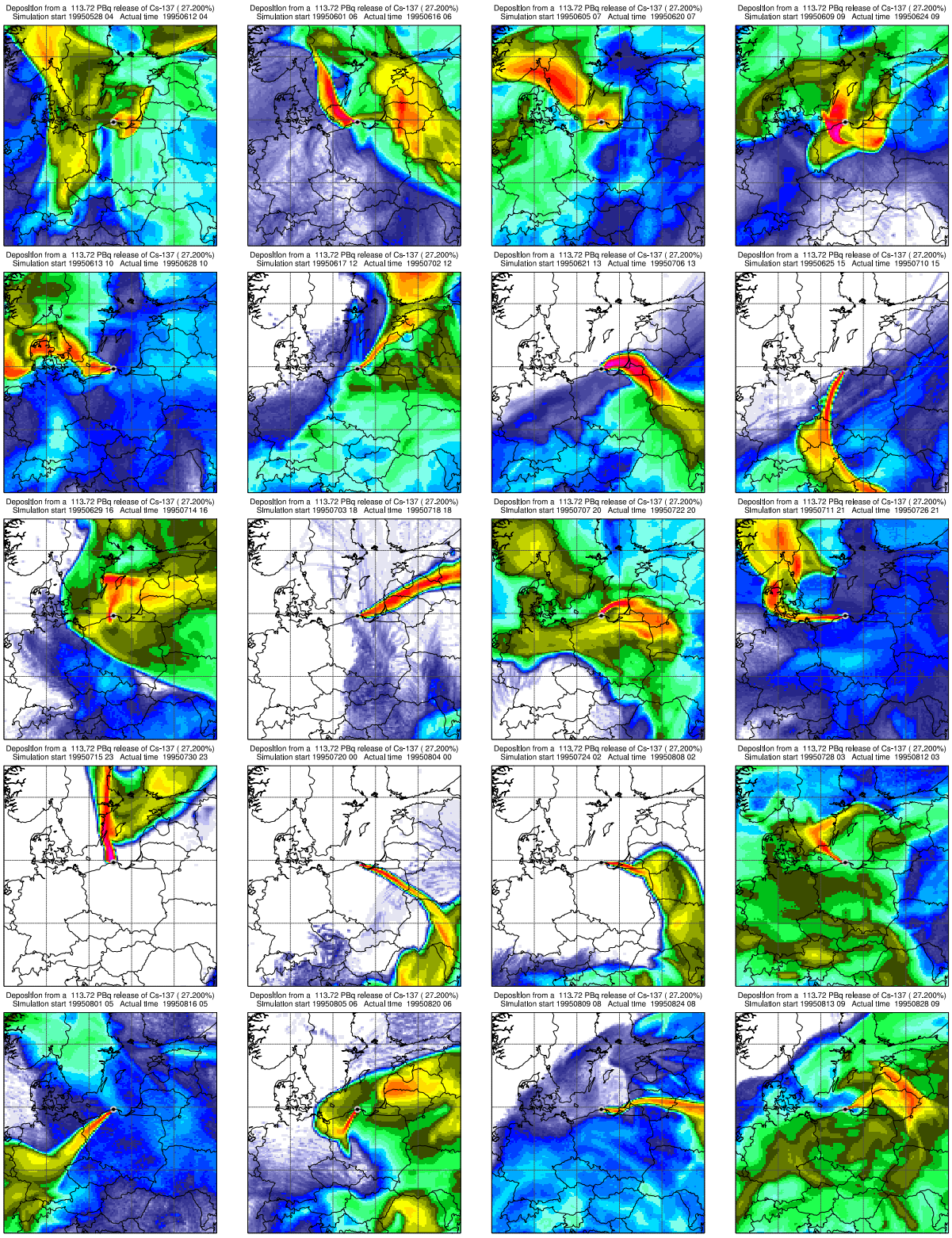
Deposition from a 113.72 PBq release of Cs-137 (27.200%)
Simulation start 19950528 04 Actual time 19950612 04
Deposition from a 113.72 PBq release of Cs-137 (27.200%)
Simulation start 19950601 06 Actual time 19950616 06
Deposition from a 113.72 PBq release of Cs-137 (27.200%)
Simulation start 19950605 07 Actual time 19950620 07
Deposition from a 113.72 PBq release of Cs-137 (27.200%)
Simulation start 19950609 09 Actual time 19950624 09
Deposition from a 113.72 PBq release of Cs-137 (27.200%)
Simulation start 19950613 10 Actual time 19950628 10
Deposition from a 113.72 PBq release of Cs-137 (27.200%)
Simulation start 19950617 12 Actual time 19950702 12
Deposition from a 113.72 PBq release of Cs-137 (27.200%)
Simulation start 19950621 13 Actual time 19950706 13
Deposition from a 113.72 PBq release of Cs-137 (27.200%)
Simulation start 19950625 15 Actual time 19950710 15
Deposition from a 113.72 PBq release of Cs-137 (27.200%)
Simulation start 19950629 16 Actual time 19950714 16
Deposition from a 113.72 PBq release of Cs-137 (27.200%)
Simulation start 19950703 18 Actual time 19950718 18
Deposition from a 113.72 PBq release of Cs-137 (27.200%)
Simulation start 19950707 20 Actual time 19950722 20
Deposition from a 113.72 PBq release of Cs-137 (27.200%)
Simulation start 19950711 21 Actual time 19950726 21
Deposition from a 113.72 PBq release of Cs-137 (27.200%)
Simulation start 19950715 23 Actual time 19950730 23
Deposition from a 113.72 PBq release of Cs-137 (27.200%)
Simulation start 19950720 00 Actual time 19950804 00
Deposition from a 113.72 PBq release of Cs-137 (27.200%)
Simulation start 19950724 02 Actual time 19950808 02
Deposition from a 113.72 PBq release of Cs-137 (27.200%)
Simulation start 19950728 03 Actual time 19950812 03
Deposition from a 113.72 PBq release of Cs-137 (27.200%)
Simulation start 19950801 05 Actual time 19950816 05
Deposition from a 113.72 PBq release of Cs-137 (27.200%)
Simulation start 19950805 06 Actual time 19950820 06
Deposition from a 113.72 PBq release of Cs-137 (27.200%)
Simulation start 19950809 08 Actual time 19950824 08
Deposition from a 113.72 PBq release of Cs-137 (27.200%)
Simulation start 19950813 09 Actual time 19950828 09

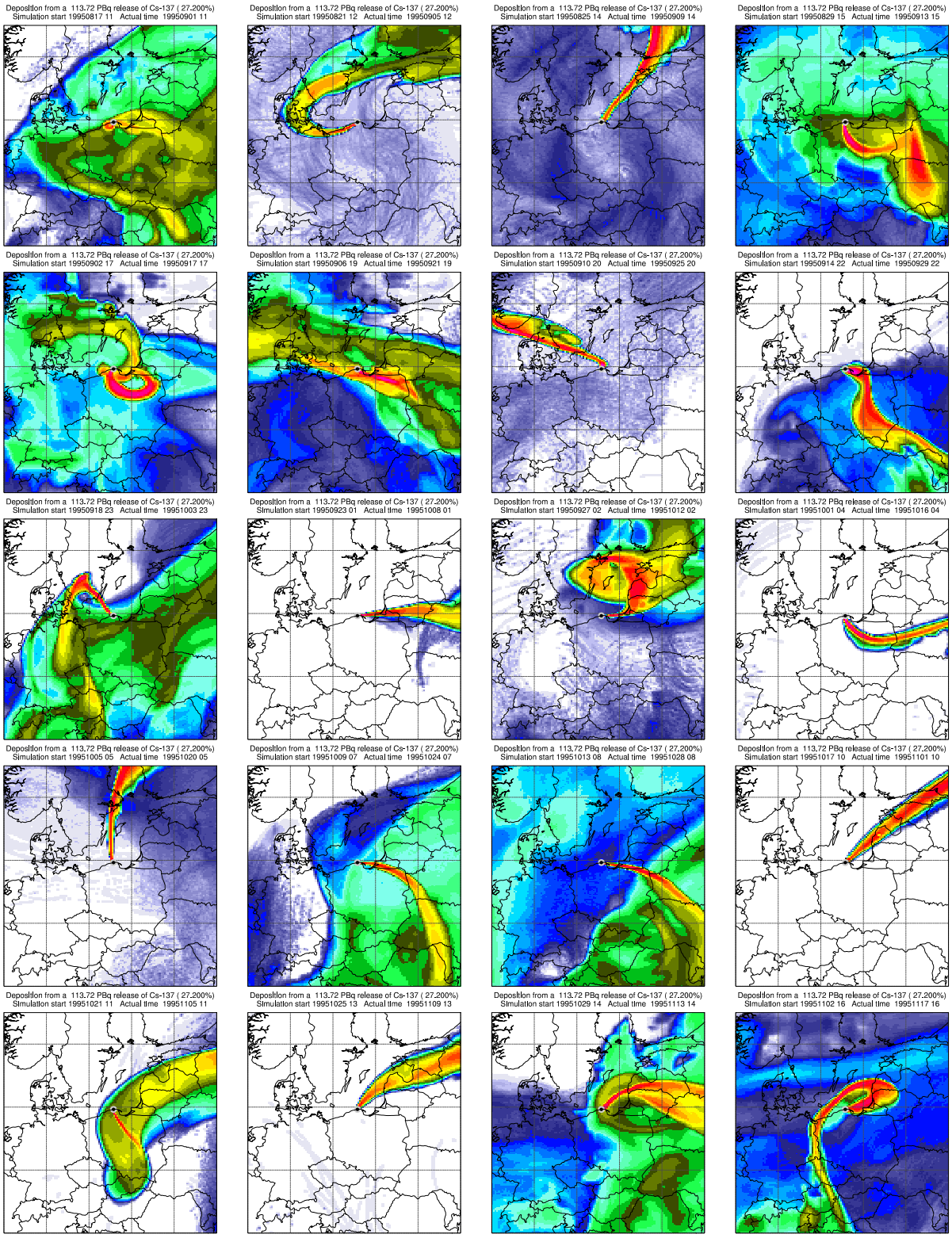
Deposition from a 113.72 PBq release of Cs-137 (27.200%)
Simulation start 19950817 11 Actual time 19950901 11
Deposition from a 113.72 PBq release of Cs-137 (27.200%)
Simulation start 19950821 12 Actual time 19950905 12
Deposition from a 113.72 PBq release of Cs-137 (27.200%)
Simulation start 19950825 14 Actual time 19950909 14
Deposition from a 113.72 PBq release of Cs-137 (27.200%)
Simulation start 19950829 15 Actual time 19950913 15
Deposition from a 113.72 PBq release of Cs-137 (27.200%)
Simulation start 19950902 17 Actual time 19950917 17
Deposition from a 113.72 PBq release of Cs-137 (27.200%)
Simulation start 19950906 19 Actual time 19950921 19
Deposition from a 113.72 PBq release of Cs-137 (27.200%)
Simulation start 19950910 20 Actual time 19950925 20
Deposition from a 113.72 PBq release of Cs-137 (27.200%)
Simulation start 19950914 22 Actual time 19950929 22
Deposition from a 113.72 PBq release of Cs-137 (27.200%)
Simulation start 19950918 23 Actual time 19951003 23
Deposition from a 113.72 PBq release of Cs-137 (27.200%)
Simulation start 19950923 01 Actual time 19951008 01
Deposition from a 113.72 PBq release of Cs-137 (27.200%)
Simulation start 19950927 02 Actual time 19951012 02
Deposition from a 113.72 PBq release of Cs-137 (27.200%)
Simulation start 19951001 04 Actual time 19951016 04
Deposition from a 113.72 PBq release of Cs-137 (27.200%)
Simulation start 19951005 05 Actual time 19951020 05
Deposition from a 113.72 PBq release of Cs-137 (27.200%)
Simulation start 19951009 07 Actual time 19951024 07
Deposition from a 113.72 PBq release of Cs-137 (27.200%)
Simulation start 19951013 08 Actual time 19951028 08
Deposition from a 113.72 PBq release of Cs-137 (27.200%)
Simulation start 19951017 10 Actual time 19951101 10
Deposition from a 113.72 PBq release of Cs-137 (27.200%)
Simulation start 19951021 11 Actual time 19951105 11
Deposition from a 113.72 PBq release of Cs-137 (27.200%)
Simulation start 19951025 13 Actual time 19951109 13
Deposition from a 113.72 PBq release of Cs-137 (27.200%)
Simulation start 19951029 14 Actual time 19951113 14
Deposition from a 113.72 PBq release of Cs-137 (27.200%)
Simulation start 19951102 16 Actual time 19951117 16

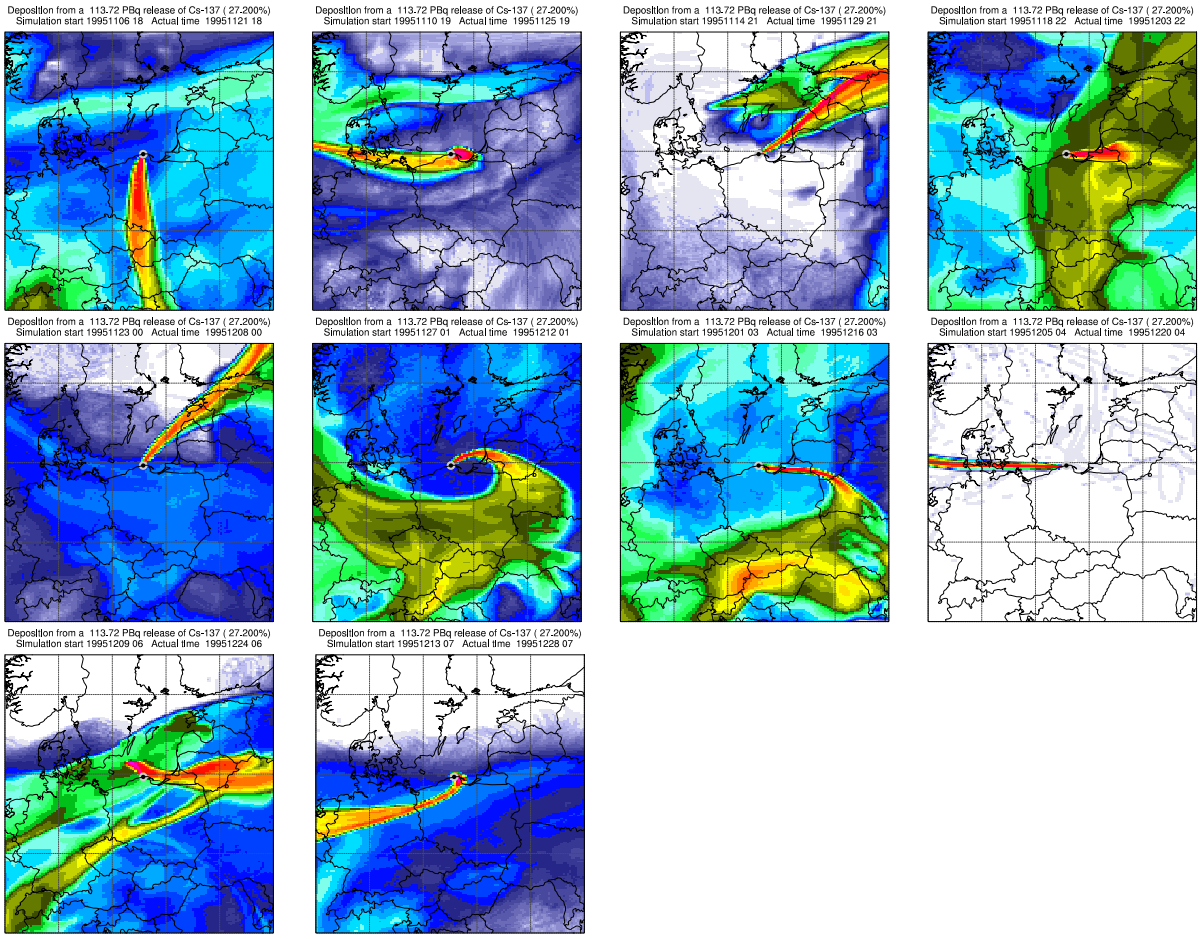

5.4.2 Discussion of some selected cases

Three cases are selected which are associated with major consequences for Polish cities. Maximum dose values have been extracted for the areas around the cities of Gdynia, Gdańsk, and Warszawa (Warsaw) which are shown in Figure 5. They will be discussed in more detail.

Table 10: Maximum doses within the boxes shown in Fig. 5 for selected sites and cases. Consider the different assumptions on pathways and shielding!

Dose type	Age group	Gdańsk (mSv)	Gdynia (mSv)	Warsaw (mSv)
thyroid 7 d	infants	477	7531	195
	adults	395	5640	154
effective 7 d	infants	58	862	16
	adults	49	993	14
effective 30 d	infants	116	156	12
	adults	78	104	8
effective 1 a	infants	880	853	41
	adults	592	793	29
effective 50 a	infants	5836	2279	202
	adults	3479	1638	123

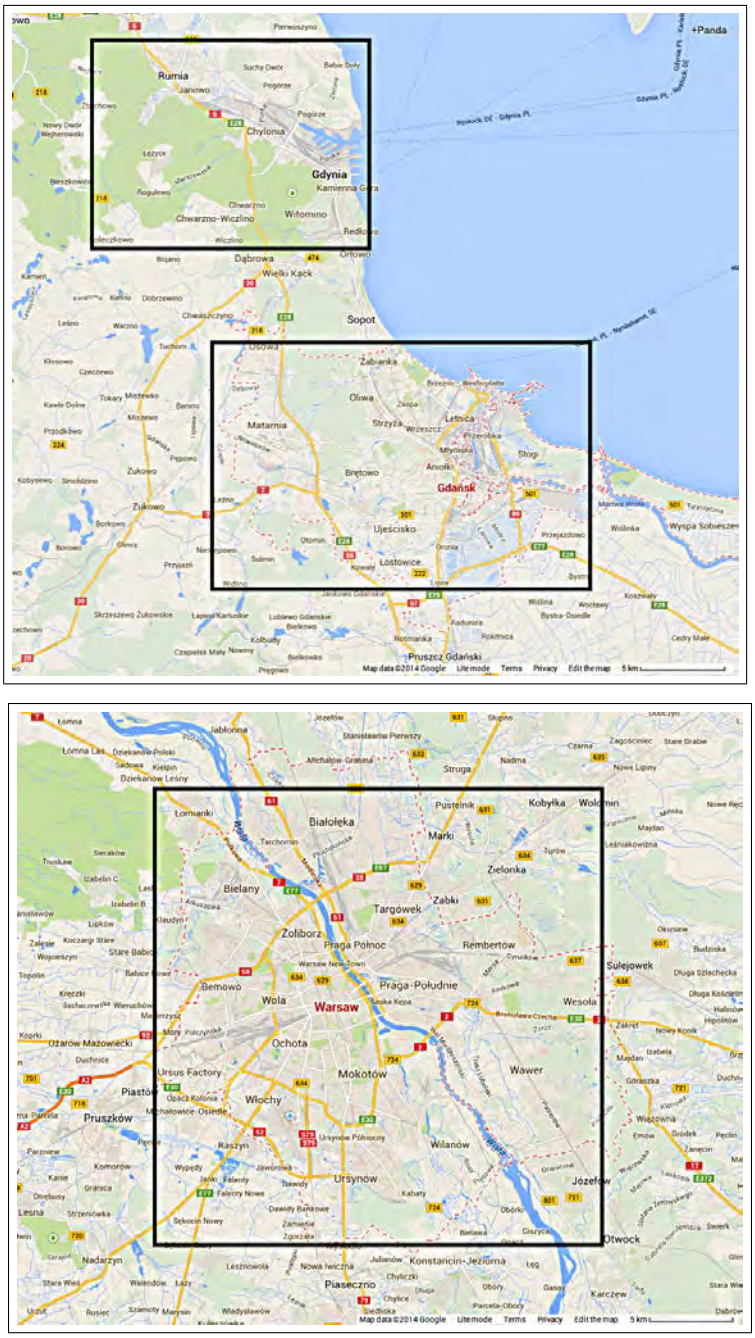

Figure 5: Selection boxes for Gdynia and Gdańsk, and Warsaw.

Case 1 assumes a release on 02 Sept 1995 at 17 UTC, and the accident 3B is considered. Figure 6 shows contamination and dose maps for this case.

This is the largest release, almost 300 PBq ^{137}Cs and 2 EBq ^{131}I. Consequently, a trace of very high ^{137}Cs deposition below the plume centerline extends southeaseward, with contamination maxima on the order of 10 MBq m^{-2}. About 30% of the Polish territory (northeastern part) would be contaminated with more than 500 or 1000 kBq m^{-2}. This would have massive consequences – after Chernobyl, population was relocated from such areas. In most of this region, the 50 mSv thyroid dose limit would be exceeded for infants (for adults in an area which is a

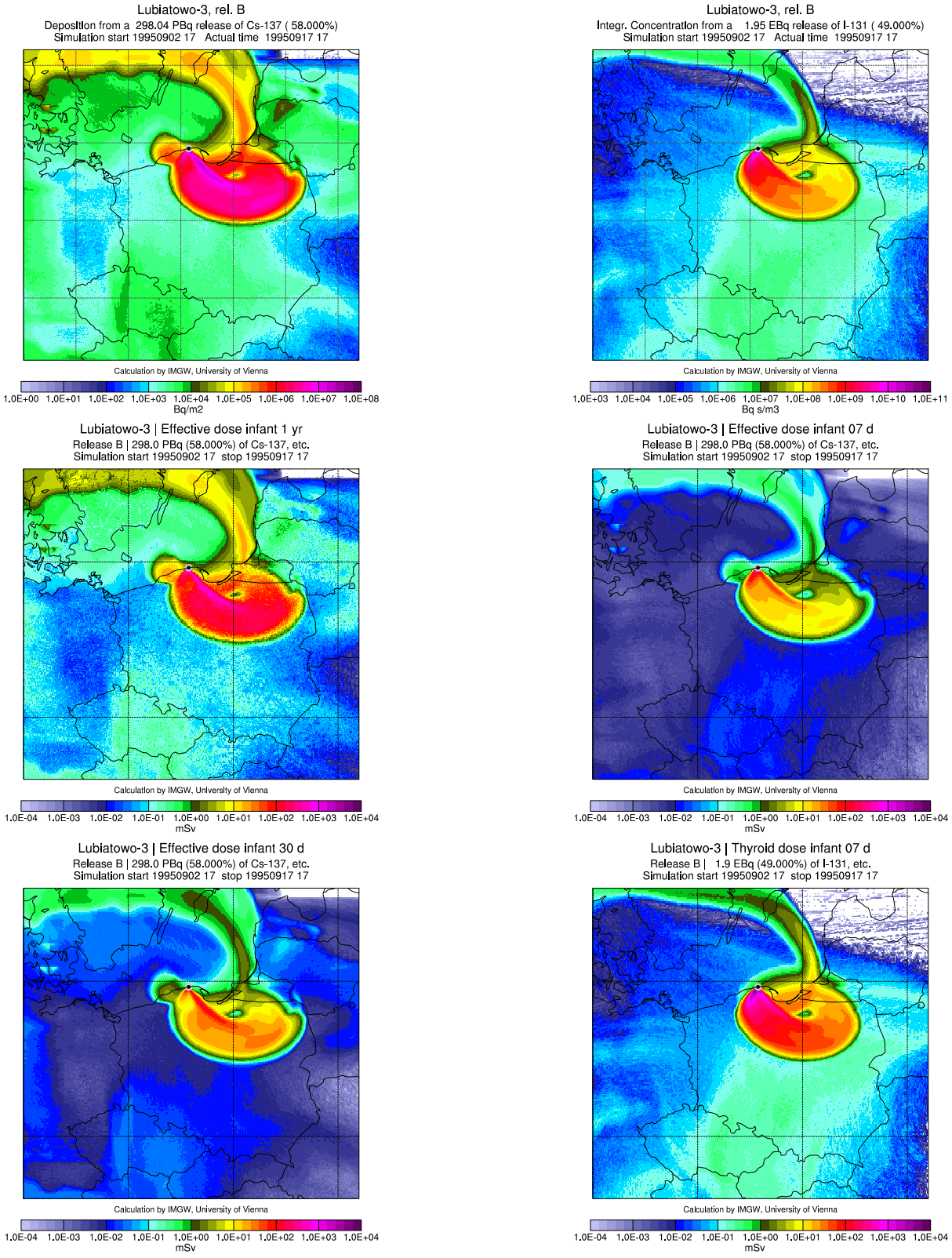

Figure 6: Contamination and dose for Case 1 (release 02 Sept 1995 at 17 UTC, accident 3B). Panels show, by row: deposition of ^{137}Cs; integrated air concentration of ^{131}I; 1-year effective dose infants (all pathways, shielding considered; 7-days effective dose infants, groundshine only, no shielding; 30-days effective dose infants, all pathways, no shielding; 7-days thyroid dose, infants, not shielding.

bit smaller, not shown). Effective doses for the 7 d and 30 d periods would exceed intervention limits for sheltering and temporary relocation (here taken the Austrian standards, with other standards there may be some modifications) along the main plume in distances on the order of 100 km.

The concentrated plume would just pass along the western parts of the city of Gdańsk.

Case 2 assumes a release on 06 Sept 1995 at 19 UTC, and the accident 2B is considered. Figure 7 shows contamination and dose maps for this case.

The release in this case is smaller, but still quite large (163 PBq ^{137}Cs, 915 PBq ^{131}I). The contaminted areas would be a bit more concentrated and extend along the northern border of Poland into western Byelorussia. The radioactive cloud would firstmove towards the east-southeast and then, undergoing strong deformation, move backward. Extremely high air concentrations and thus thyroid as well as effective doses would occur southeast of the site and cross the city of Gdynia. Intervention measures such as iodine prophylaxis would be recommendable even in Western Byelorussia.

Case 3 assumes a release on 14 Sept 1995 at 22 UTC, and the accident 3B is considered. Figure 8 shows contamination and dose maps for this case.

This release is also very large (114 PBq ^{137}Cs, 1.6 EBq ^{131}I). The meteorological situation is such that the radioactive cloud first travels east, then south towards Warsaw, passing just west of the city centre, and then turns east again. All along this path, heavy contamination occurs. The 500 kBq Cs-137 m^{-2} zone reaches the Ukrainian border. Infant thyroid doses exceed the 50 mSv limit across the whole country of Poland, including Warsaw. In the border region to the Kaliningrad territory, about 500 mSv are reached, and in the near surrounding of the site even 1 Sv is exceeded.

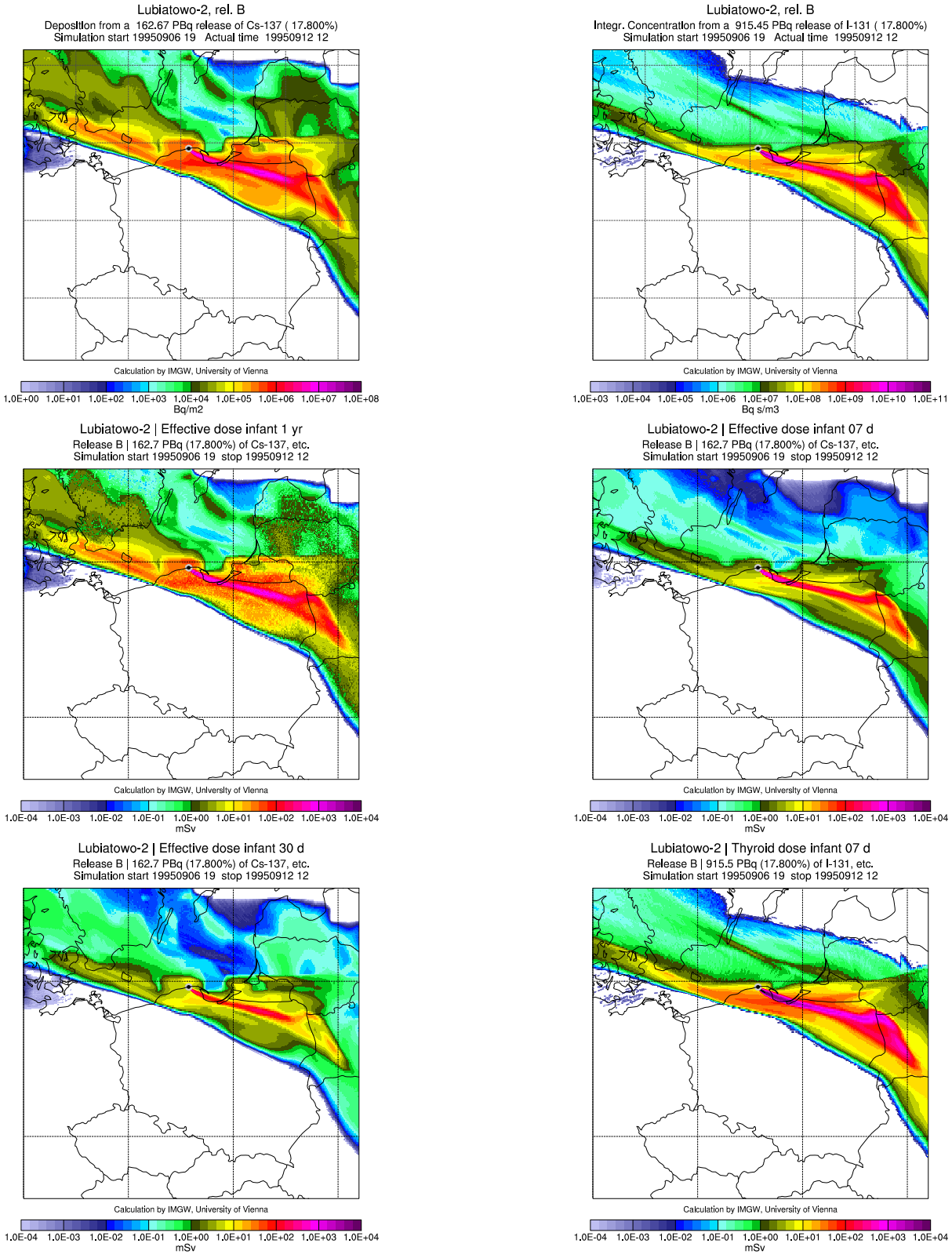

Figure 7: Contamination and dose for Case 1 (release 06 Sept 1995 at 19 UTC, accident 2B). Panels show, by row: deposition of ^{137}Cs; integrated air concentration of ^{131}I; 1-year effective dose infants (all pathways, shielding considered; 7-days effective dose infants, groundshine only, no shielding; 30-days effective dose infants, all pathways, no shielding; 7-days thyroid dose, infants, not shielding.

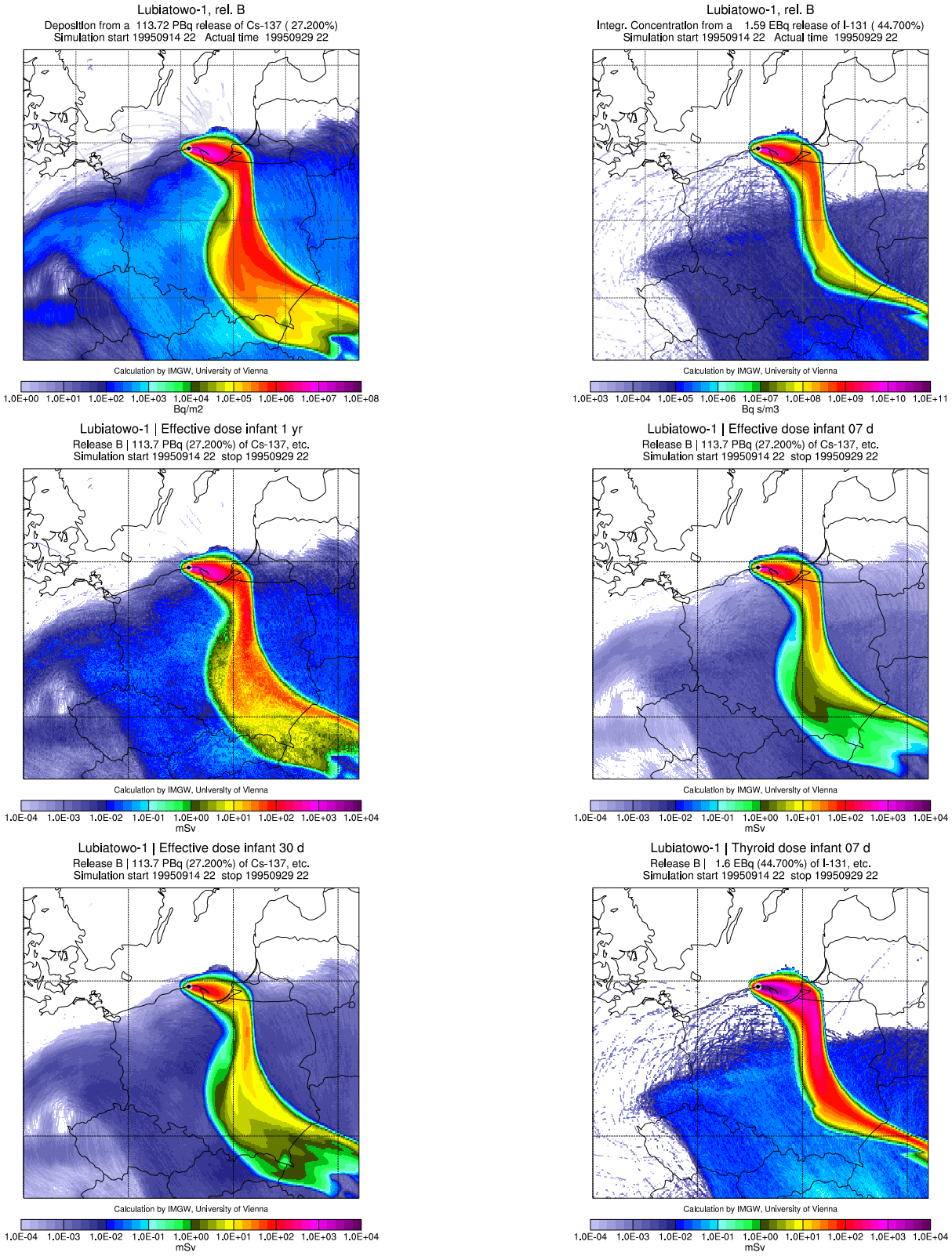

Figure 8: Contamination and dose for Case 3 (release 14 Sept 1995 at 22 UTC, accident 1B). Panels show, by row: deposition of ^{137}Cs; integrated air concentration of ^{131}I; 1-year effective dose infants (all pathways, shielding considered; 7-days effective dose infants, groundshine only, no shielding; 30-days effective dose infants, all pathways, no shielding; 7-days thyroid dose, infants, not shielding.

6 Conclusions

A state-of-the-art Lagrangian dispersion model, suitable for regional and large-scale dispersion calculations, has been used to simulate the transport, dispersion and deposition of hypothetical radioactive releases at the proposed nuclear power plant site Lubiatowo, Poland. Source terms had been defined by the Institute of Safety and Risk Research, University of Natural Resources and Life Science, Vienna. They are based on three reactor designs, and for each design cover a core-melt accident with containment intact and not bypassed, and another one with very large releases through damaged or bypassed containment. Consequences have been calculated in terms of ground and air contamination as well as various dose parameters which are commonly used for deciding about intervention measures.

In this Report, we do not investigate the consequences within a typical emergency planning zone of ca. 15 km radius. Even withouth specific calculations it is clear that in the case of the more severe type of the releases considered here, with suitable weather situations, consequences in this area will be massive and evacuations would be needed.

Outside of this area, in the case of the weaker releases, expected doses will remain below intervention limits. However, it is not excluded that if the ingestion pathway, which was not included in the present study for methodological reasons, would be considered, the regular 1-year dose limit for the general population is exceeded.

For the very severe releases, which assume source terms on the order of 100 or more PBq for ^{137}Cs and of 1000 PBq (1 EBq) for ^{131}I, consequences triggering intervention measures are possible all over Poland and even in other countries. Iodine prophylaxis is the intervention measure that is most likely even at large distances.

For the cities of the Gdynia–Gdańsk area, at a distance of 50 to 100 km from the site, adverse meteorological conditions could cause very high doses, which could trigger other measures such as sheltering or even relocation of the population. With a potential for ground contamination exceeding 1,000 kBq Cs-137 m^{-2}, the possibility of long-term loss of land for agricultural use or human settlement exists.

In the region of Warsaw, at a distance of about 300 km, iodine prophylaxis for children and adults is a possible countermeasure that could be triggered. Contamination of the ground may exceed 100 kBq Cs-137 m^{-2}, with corresponding agricultural measures, and probably also recommendations such as not to let children play on the ground etc., even though for such measures there are no detailed intervention guidelines.

Summing up, the possibility of very large releases, even if their frequencies are estimated to be extremely small, leads to correspondingly serious potential consequences.

References

Andreev, I., H. Gohla, M. Hittenberger, P. Hofer, W. Kromp, H. Kromp-Kolb, W. Rehm, P. Seibert, and G. Wotawa (1999), Riskmap – Erstellung einer Karte des nuklearen Risikos für Europa. Riskmap – Creation of a Map of the Nuclear Risk for Europe. URL: http://www.umweltbundesamt.at/umweltschutz/kernenergie/akw/riskmap/.

Andreev, I., M. Hittenberger, P. Hofer, W. Kromp-Kolb, P. Seibert, and G. Wotawa (1998), Risks due to beyond design base accidents of nuclear power plants in Europe – the methodology of Riskmap. *J. Hazardous Materials* **61**, 257–262.

Arnold, D., C. Maurer, G. Wotawa, R. Draxler, K. Saito, and P. Seibert (2014), Influence of the meteorological input on the atmospheric transport modelling with FLEXPART of radionuclides from the Fukushima Daiichi nuclear accident. *J. Environ. Radioactivity* (accepted).

Arnold, D., P. Seibert, H. Nagai, G. Wotawa, P. Skomorowski, K. Baumann-Stanzer, E. Polreich, M. Langer, A. Jones, M. Hort, S. Andronopoulos, J. G. Bartzis, E. Davakis, P. Kaufmann, and A. Vargas (2013), Lagrangian models for nuclear studies: Examples & applications. In: J. C. Lin, D. Brunner, C. Gerbig, A. Stohl, A. Luhar, and P. Webley (eds.), *Lagrangian Modeling of the Atmosphere*, vol. 26 of *AGU Geophysical Monograph*, American Geophysical Union. doi:10.1029/2012GM001294.

Bossew, P., T. Falkner, E. Henrich, and K. Kienzl (1996), Cäsiumbelastung der Böden Österreichs. Wien: Umweltbundesamt Monographien, Bd. 60, 93 pp. URL: http://www.umweltbundesamt.at/fileadmin/site/publikationen/M060.pdf.

Brioude, J., D. Arnold, A. Stohl, M. Cassiani, D. Morton, P. Seibert, W. Angevine, S. Evan, A. Dingwell, J. D. Fast, R. C. Easter, I. Pisso, J. Burkhart, and G. Wotawa (2013), The Lagrangian particle dispersion model FLEXPART-WRF version 3.1. *Geosci. Model Dev.* **6** (6), 1889–1904. URL: http://www.geosci-model-dev.net/6/1889/2013/, doi:10.5194/gmd-6-1889-2013.

Bundeskanzleramt, Sektion VII (1988), Die Auswirkungen des Reaktorunfalls in Tschernobyl auf Österreich. Wien: Beiträge Lebensmittelangelegenheiten, Veterinärverwaltung, Strahlenschutz, 291 pp.

Davoine, X. and M. Bocquet (2007), Inverse modelling-based reconstruction of the Chernobyl source term available for long-range transport. *Atmos. Chem. Phys.* **7** (6), 1549–1564. URL: http://www.atmos-chem-phys.net/7/1549/.

Dee, D. P., S. M. Uppala, A. J. Simmons, P. Berrisford, P. Poli, S. Kobayashi, U. Andrae, M. A. Balmaseda, G. Balsamo, P. Bauer, P. Bechtold, A. C. M. Beljaars, L. van de Berg, J. Bidlot, N. Bormann, C. Delsol, R. Dragani, M. Fuentes, A. J. Geer, L. Haimberger, S. B. Healy, H. Hersbach, E. V. Hólm, L. Isaksen, P. Kållberg, M. Köhler, M. Matricardi, A. P. McNally, B. M. Monge-Sanz, J.-J. Morcrette, B.-K. Park, C. Peubey, P. de Rosnay, C. Tavolato, J.-N. Thépaut, and F. Vitart (2011), The ERA-Interim reanalysis: configuration and performance of the data assimilation system. *Q. J. Royal Meteorol. Soc.* **137**, 553–597. URL: http://dx.doi.org/10.1002/qj.828, doi:10.1002/qj.828.

FLEXPART Developer Team (no date), FLEXPART web site. URL: http://flexpart.eu/.

flexRISK team (no date), flexRISK – Flexible tools for assessment of nuclear risk in Europe. Website. URL: http://flexrisk.boku.ac.at/.

Forster, C., A. Stohl, and P. Seibert (2007), Parameterization of convective transport in a Lagrangian particle dispersion model and its evaluation. *J. Climate Appl. Meteorol.* **46**, 403–422. URL: http://journals.ametsoc.org/doi/abs/10.1175/JAM2470.1, doi:10.1175/JAM2470.1.

Hofer, P., P. Seibert, I. Andreev, H. Gohla, and H. Kromp-Kolb (2000), Risks due to severe accidents of nuclear power plants in Europe – the methodology of Riskmap. In: *Transitions Towards a Sustainable Europe. Ecology–Economy–Policy*, 3rd Biennial Conference of the European Society for Ecological Economics, Vienna. URL: http://www.wu.ac.at/project/esee2000/PapersPDF/C316.pdf.

IAEA (2011), Criteria for use in preparedness and response for a nuclear or radiological emergency. IAEA Safety Standards, General Safety Guide No. GSG-2, jointly sponsored by the FAO, IAEA, ILO, PAHO, WHO, Vienna.

ICRP (1991), Recommendations of the International Commission on Radiological Protection. Annals of the ICRP 21(1-3). ICRP Publication 60. Pergamon Press, Oxford.

Lebensministerium (2007), Verordnung des Bundesministers für Land- und Forstwirtschaft, Umwelt und Wasserwirtschaft über Interventionen bei radiologischen Notstandssituationen und bei dauerhaften Strahlenexpositionen (Interventionsverordnung – IntV). Bundesgesetz BGBl. II Nr. 145/2007, ausgegeben am 26. Juni 2007. URL: http://www.lebensministerium.at/umwelt/strahlen-atom/strahlenschutz/rechtsvorschriften/intV.html.

Seibert, P., D. Arnold, N. Arnold, K. Gufler, H. Kromp-Kolb, G. Mraz, S. Sholly, and A. Wenisch (2013), Flexrisk – Flexible tools for assessment of nuclear risk in Europe. Final Report. PRELIMINARY VERSION MAY 2013. URL: http://www.boku.ac.at/met/report/BOKU-Met_Report_23_PRELIM_online.pdf.

Seibert, P., D. Arnold, G. Mraz, N. Arnold, K. Gufler, H. Kromp-Kolb, W. Kromp, P. Sutter, and A. Wenisch (2012), Severe accidents of nuclear power plants in Europe: Possible consequences and mapping of risk. In: Marc Stal, Manuela Stiffler, Walter Ammann (eds.), IDRC Davos 2012 International Disaster and Risk Conference, Extended Abstracts, Global Risk Forum GRF Davos, Switzerland. URL: http://www.slideshare.net/GRFDavos/severe-accidents-of-nuclear-power-plants-in-europe-possible-consequences-and-mapping-of-risk.

Seibert, P. and A. Philipp (2013), The role of deposition in atmospheric transport of radionuclides. Poster at the CTBTO Science and Technology Conference, 17-21 June 2013. URL: http://homepage.univie.ac.at/petra.seibert/files/posterCTBTO2013_wetdepo.pdf.

Shevchik, V. E. and V. L. Gurachevsky (2006), National Report Belarus: 20 years after the Chernobyl catastrophe: The consequences in the Republic of Belarus and their overcoming. Committee on the Problems of the Consequences of the Catastrophe at the Chernobyl NPP under the Belarussian Council of Ministers, Minsk. URL: http://chernobyl.undp.org/english/nat_rep.shtml.

Sholly, S., N. Müllner, N. Arnold, and K. Gufler (2014), Source terms for potential NPPs at the Lubiatowo site, Poland. Report prepared for Greenpeace Germany, Institut für Sicherheits- und Risikowissenschaften, BOKU Wien.

SSK (2008), Radiologische Grundlagen für Entscheidungen über Maßnahmen zum Schutz der Bevölkerung bei unfallbedingten Freisetzungen von Radionukliden. Empfehlung der Strahlenschutzkommission. Redaktionelle Überarbeitung der gleichnamigen Veröffentlichung aus dem Jahr 1999. Stand 21.09.2008.

Stohl, A., C. Forster, A. Frank, P. Seibert, and G. Wotawa (2005), Technical note: The Lagrangian particle dispersion model FLEXPART version 6.2. *Atmos. Chem. Phys.* **5**, 2461–2474. URL: http://www.atmos-chem-phys.net/5/2461/2005/.

Stohl, A., M. Hittenberger, and G. Wotawa (1998), Validation of the Lagrangian particle dispersion model Flexpart against large-scale tracer experiment data. *Atmos. Environ.* **32** (24), 4245–4264.

Stohl, A., P. Seibert, G. Wotawa, D. Arnold, J. F. Burkhart, S. Eckhardt, C. Tapia, A. Vargas, and T. J. Yasunari (2012), Xenon-133 and caesium-137 releases into the atmosphere from the Fukushima Dai-ichi nuclear power plant: determination of the source term, atmospheric dispersion, and deposition. *Atmospheric Chemistry and Physics* **12** (5), 2313–2343. URL: http://www.atmos-chem-phys.net/12/2313/2012/, doi:10.5194/acp-12-2313-2012.

Stohl, A., H. Sodemann, E. S., A. Frank, P. Seibert, and G. Wotawa (2010), The Lagrangian particle dispersion model FLEXPART version 8.2. 32 pp. URL: http://zardoz.nilu.no/~flexpart/flexpart/flexpart82.pdf.

Wenzel, H., M. Brettner, P. Seibert, B. Theilen-Willige, H. Allmer, M. Höllrigl-Binder, D. Arnold, T. Gorgas, H. Kromp-Kolb, and G. Mraz (2012), KKW Mühleberg. Fachstellungnahme zu sicherheitstechnischen Aspekten des Schweizer Kernkraftwerkes Mühleberg. Erstellt im Auftrag des Bundesministeriums für Land- und Forstwirtschaft, Umwelt und Wasserwirtschaft, Abteilung V/6 Nuklearkoordination, 335 S. + 2 Anhänge. URL: http://www.umweltbundesamt.at/umweltsituation/kernenergie/akw/kkwmuehleberg/.